

Supporting Information

Nanoelectrode-mediated Single Neurons Activation

*Juyoung Kwon[†], Sukjin Ko[‡], Jaejun Lee[†], Jukwan Na[†], Jaesuk Sung[†], Hyo-Jung Lee[†],
Seonghyeon Lee[†], Seungsoo Chung^{*‡}, and Heon-Jin Choi^{*†}*

[†]Department of Materials Science and Engineering, Yonsei University, Seoul 03722, Republic of Korea.

[‡] Brain Korea 21 Plus Project for Medical Science, Department of Physiology, Yonsei University College of Medicine, Seoul 03722, Republic of Korea.

*Corresponding Authors. E-mail: sschung@yuhs.ac and hjc@yonsei.ac.kr

Device fabrication

Samples were prepared from an intrinsic Si (111) wafer. They were first cleaned with acetone and ethanol and coated with photoresist, and the disc array pattern was transferred to the resist layer using a standard photolithography technique. After development and rinsing in isopropyl alcohol (IPA), the samples were treated briefly with oxygen plasma to remove any resist residues from the exposed areas. After plasma treatment, they were etched for 200 s with CF_4 plasma to remove surface oxide. The samples were then immediately transferred to a vacuum chamber where a gold film was deposited (thickness ranging from 5 to 10 nm) using a sputter. After metal lift-off by dissolution of the photoresist layer in acetone for 15 min, followed by 5 min in ethanol, gold dots for the growth catalyst were obtained. The samples were then placed in a low-pressure chemical vapor deposition (CVD) chamber, and the Si nanowires (NWs) were epitaxially grown on a substrate using a vapor-liquid-solid (VLS) mechanism. The diameters, densities, and heights of the SiNWs can be controlled by the growth parameters, the size and thickness of the gold disc, and growth time, respectively. A top-down complementary metal-oxide semiconductor (CMOS) device process for nanowire electrode fabrication was reported in detail in our previous study.¹⁻³ Then, 64-stimulation pads were made independently addressed by first defining the electrode tracks using photolithography, followed by deposition of a Ti/Au layer. These tracks were then subjected to SiO_2 passivation via using a high-density plasma CVD process. Subsequently, the SiO_2 layer of NW electrodes was selectively etched out to expose the Au of the NW surface by a buffered oxide etchant. Finally, the metal contact pad at the bottom of each electrode track was wired with a Ag-wire to facilitate electrical interfacing for the stimulation set-up.

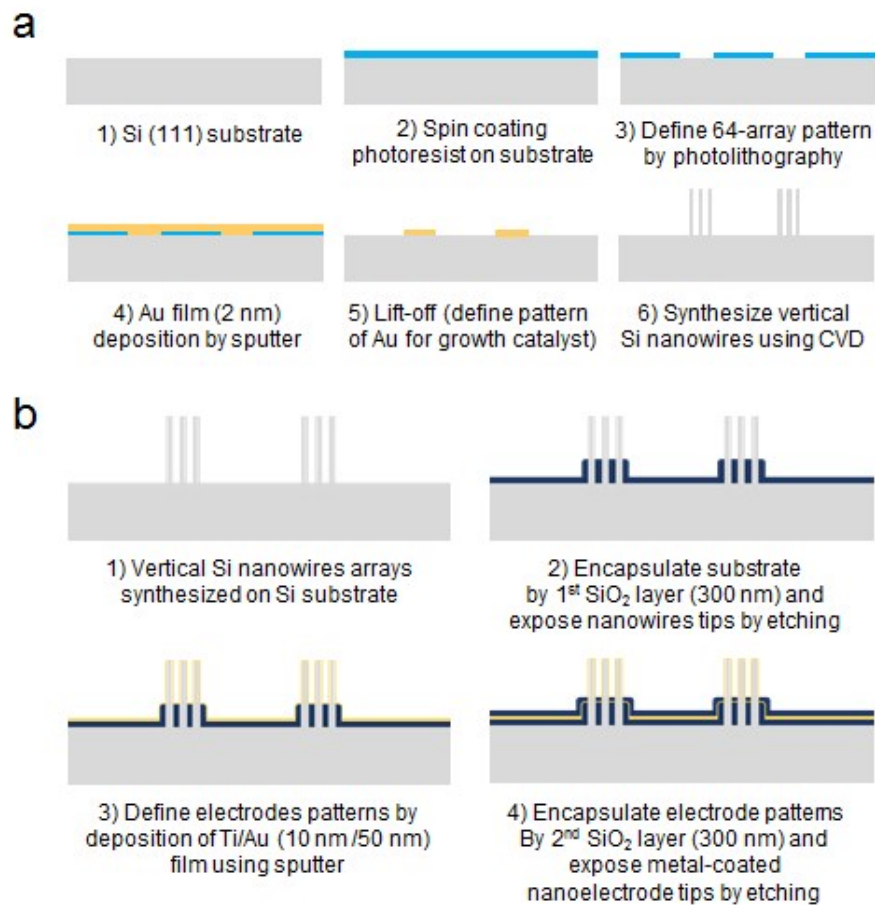


Figure S1. The VNMEA two-step fabrication process in order of ‘bottom-up nanowire synthesis’ and ‘top-down nanoelectrode fabrication process’. **a.** The bottom-up nanowire synthesis using the lithographic method. Single crystal vertical silicon nanowires are synthesized on Si (111) substrate which is patterned in 64-arrays of catalyzing gold (grey, silicon; light-blue, photoresist; yellow, gold). **b.** 64-arrays of vertically grown silicon nanowires are fabricated into nanoelectrode array using complementary CMOS top-down process (dark-blue, SiO₂; yellow, titanium/gold).

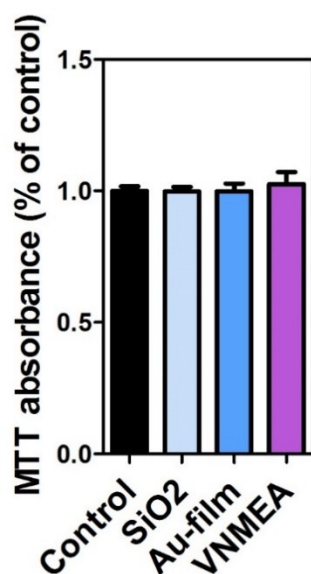


Figure S2. Normalized absorbance in the MTT cell viability test of primary hippocampal neurons, according to different substrates. Commercialized culture plates were used as a control. The absorbance was normalized against a control. The cell viability result indicates that VNMEA showed a similar biocompatibility to that of other materials.

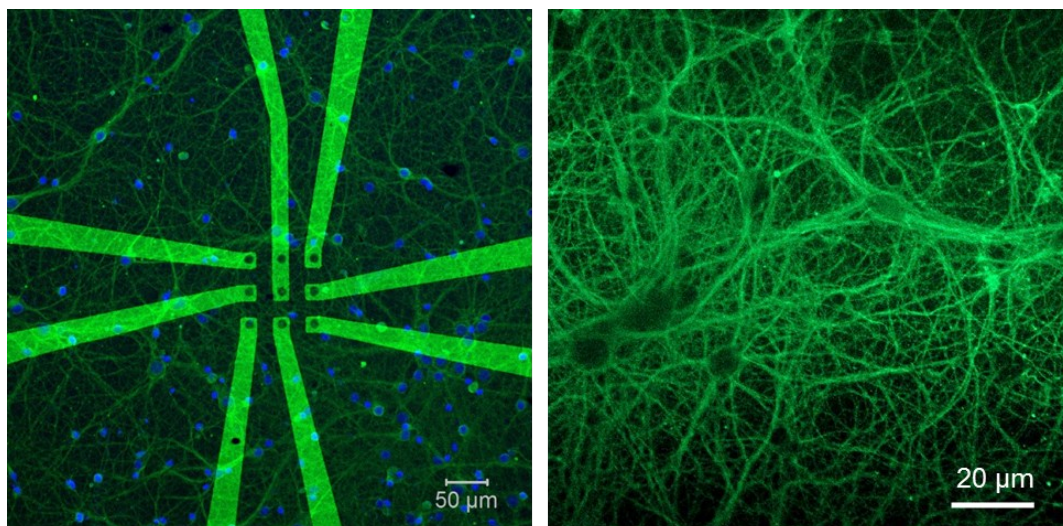


Figure S3. Immunofluorescence staining of primary hippocampal neurons cultured on VNMEA (15 DIV). Nuclear staining (DAPI) is shown in blue, with cytoplasmic staining (GFP) in green. Images demonstrate that the neurons formed typical neuronal networks on the VNMEA device.

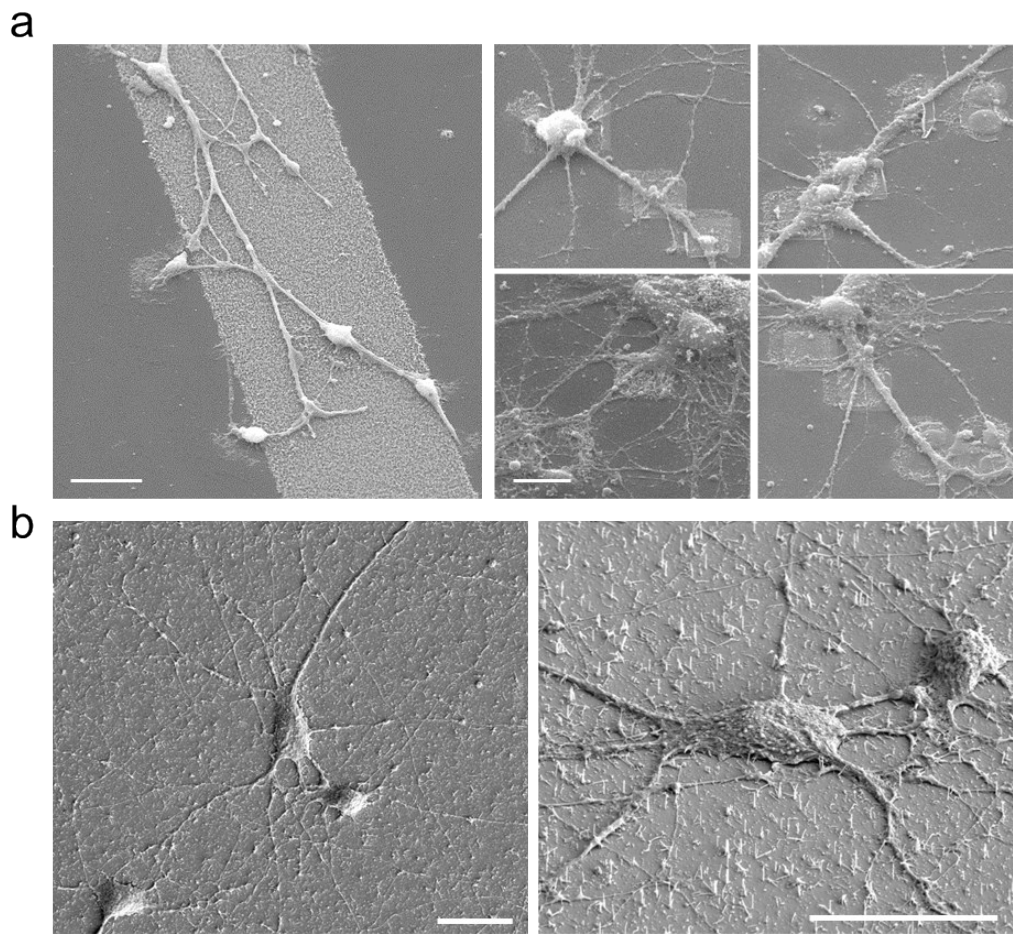


Figure S4. SEM images of primary hippocampal neurons cultured on vertical silicon nanowire array (15 DIV). a. Oriented growth of hippocampal neurons on the vertical nanowire arrays. Scale bar, 20 μm . **b.** Neurons grow unhindered and make synaptic connections with long axonal outgrowth even on the bundle of vertical Si nanowires epitaxially grown on a silicon substrate using Au colloid particles for catalyst. Scale bar, 20 μm .

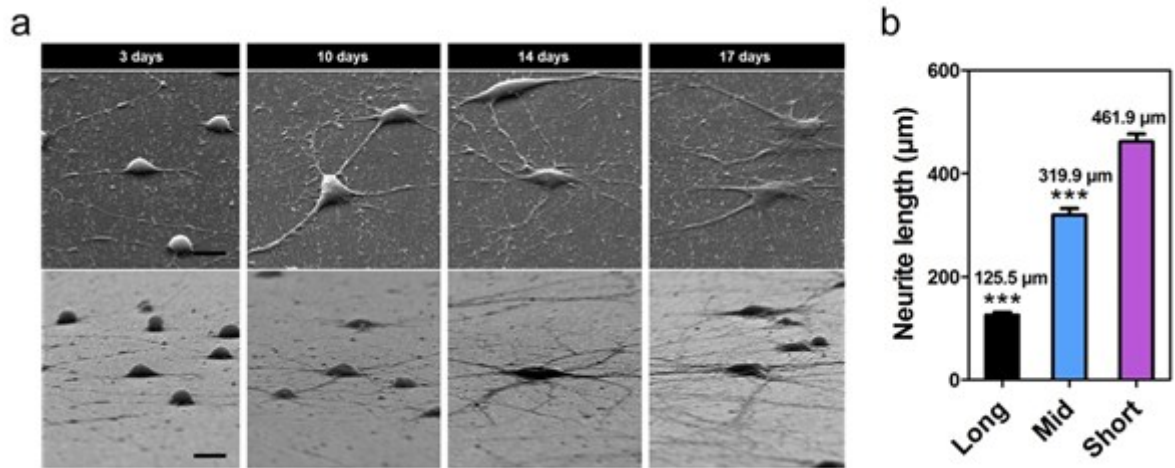


Figure S5. Optimization of nanowire height in accordance with the flattening properties of mammalian neurons. **a.** SEM images of hippocampal neurons at different culture timepoints. Images show that cells are notably flattened over time. Scale bar, 10 μm **b.** Statistical analysis of the neurite length of hippocampal neurons cultured in different nanowire heights (Long: > 5 μm, Mid: 3 ~ 5 μm, Short: < 2 μm). The statistical analysis was performed after 15 days of cell growth. All values are given as means and standard deviation, as determined by t-test. *** statistical difference compared to cells cultured in short nanowires ($p < 0.001$ for all statistical comparisons and performed on 100 samples of neurite length in each condition).

Modeling of membrane current induced by nanoelectrode-mediated intracellular stimulation

We mathematically describe the computational model of membrane conductance during the intracellular current stimulation by VNMEA based on Hodgkin-Huxley formalism. This model consists of membrane capacitance, nonlinear conductances for sodium ions (Na^+) and potassium ions (K^+), and a linear leakage element due to chloride (Cl^-) and other ions. To combine the capacitance and conductance parallelly, we express the total membrane current with capacity current, ionic current and the stimulating current by VNMEA. The current through membrane can be expressed by

$$I = C_M \frac{dV}{dt} + I_{ion} + I_{VNMEA}$$

where I is the membrane current density; C_M is the membrane capacitance per unit area; V is the value of the resting potential; t is time; I_{ion} is the ionic current density; and I_{VNMEA} is the injected current from VNMEA. The linear ionic conductance is defined by

$$I_{ion} = \sum_i g_i (V - V_i) \quad (i = Na, K, Cl)$$

where g_{Na} , g_K , and g_{Cl} are the ionic conductances; and V_{Na} , V_K , and V_{Cl} are the ionic Nernst potentials. While the g_{Cl} conductance is linear, the g_{Na} and g_K conductances are complex nonlinear functions of the form

$$g_{Na} = \bar{g}_{Na} m^3 h$$

$$g_K = \bar{g}_K n^4$$

Therefore, we may express the total membrane current I including the membrane intrinsic capacity current, ionic current, and the stimulating current from VNMEA during the intracellular stimulation as a function of time and voltage. These are:

$$I = C_M \frac{dV}{dt} + \bar{g}_{Na} m^3 h (V - V_{Na}) + \bar{g}_K n^4 (V - V_K) + \bar{g}_{Cl} (V - V_{Cl}) + I_{VNMEA}$$

This quantitative expression of membrane conductance in generic neuron model describes the effect of the intracellular current injection by VNMEA in generic neurons which have function of voltage- and time-dependent activation.

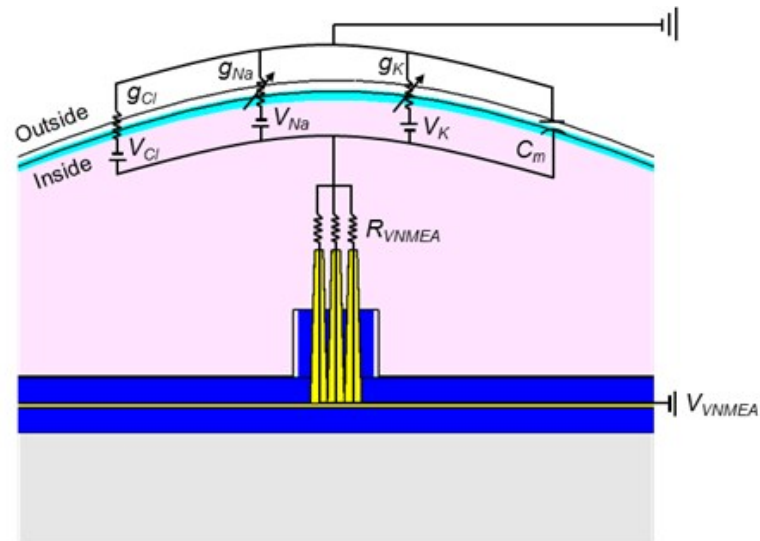


Figure S6. Equivalent electrical circuit of generic neuron model interacted with nanoelectrode in this study based on Hodgkin-Huxley formalism. V_{VNMEA} , applied voltage in VNMEA nanoelectrode; R_{VNMEA} , nanoelectrode resistance; C_m , membrane capacitance, g_{Na} , voltage-dependent sodium ion conductance; g_K , voltage-dependent potassium ion conductance; g_{Cl} , chloride and other ion leakage conductance; V_{Na} and V_K , the equilibrium potentials from the sodium and potassium ions, respectively; V_{Cl} , ionic potential at which the leakage current due to chloride and other ions. The voltage sources (V_{Na} , V_K , and V_{Cl}) are the Nernst equilibrium potentials associated with each channel type according to the concentration gradient across the neuronal membrane of each ion. The current applied intracellularly by VNMEA nanoelectrode is directly delivered into the cell interior and induced the change of transmembrane potential excluding the resistivity and capacitance of cell membrane.

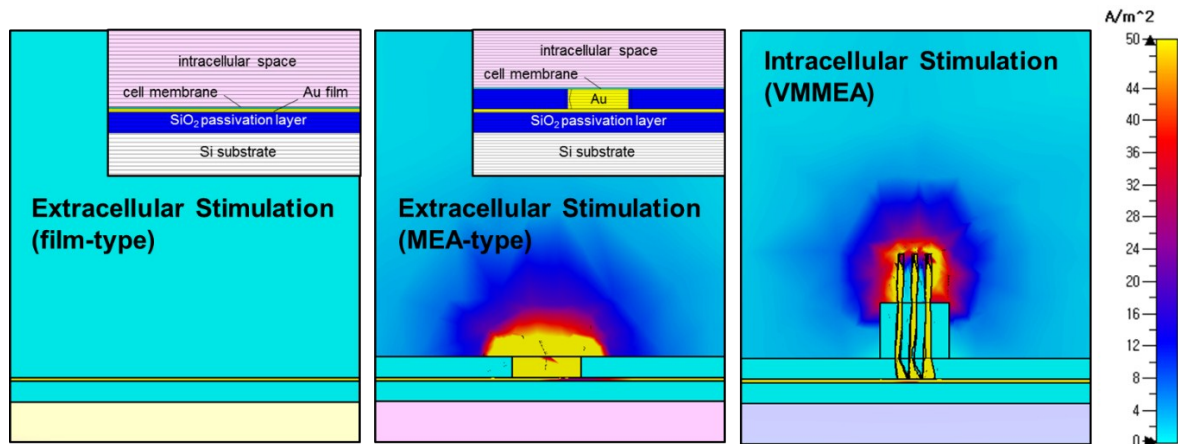


Figure S7. Tendency of electrical focusing according to the geometrical property of the electrode. Current density distribution is focused on the narrowing the electrode shape gradually increasing in the following order: film-type, MEA-type, and VNMEA-type electrode. Superior activation property of VNMEA-based intracellular stimulation is based on not only the location of the electrode inside of cell membrane but also its three-dimensional geometrical property.

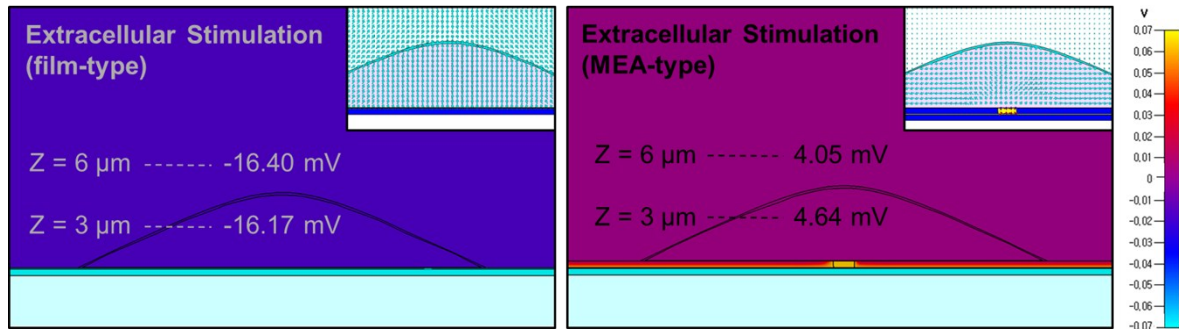


Figure S8. Extracellular electrical effects of the cells according to the geometrical property of electrodes (film-type and MEA-type). The same tendency of electrical focusing according to geometrical property of electrodes is also observed in application to cells. The increase of potential difference and current density focusing is observed in MEA-type electrode compared to film-type electrode. (For transmembrane potential, film-type electrode, 0.23 mV; MEA-type electrode, 0.59 mV, For current density, film-type, 1.0×10^{-3} A/m²; MEA-type, 42.5×10^{-3} A/m²).

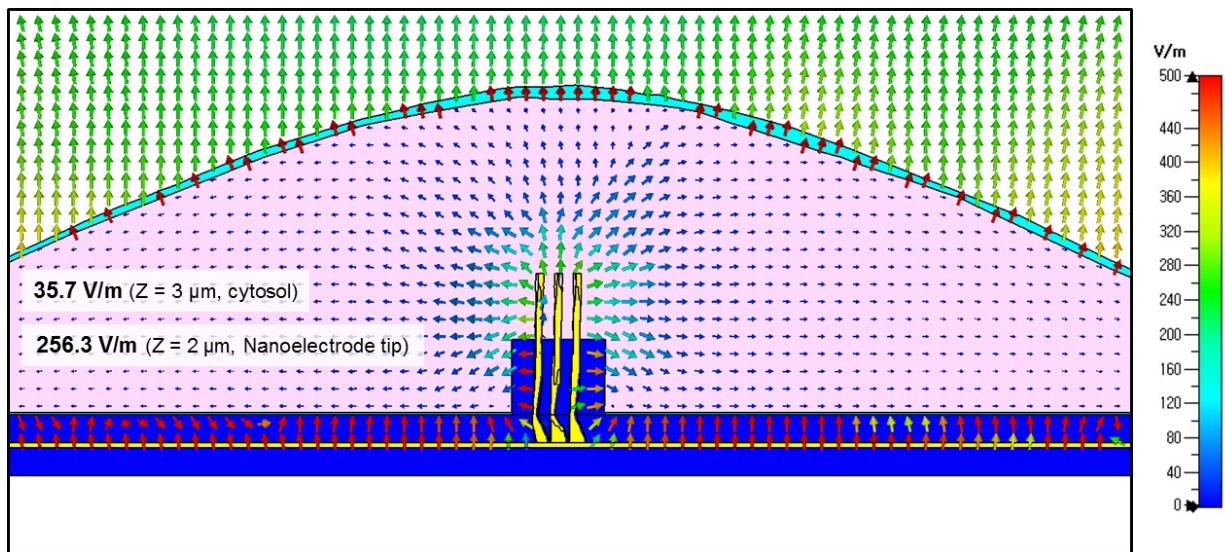


Figure S9. Electric field induced in neurons during the intracellular stimulation by VNMEA. During the intracellular stimulation, the electric field strength induced in single neuron is 35.7 V/m at 3 μm height in cytosol and 256.3 V/m at 2 μm height of nanoelectrode tip.

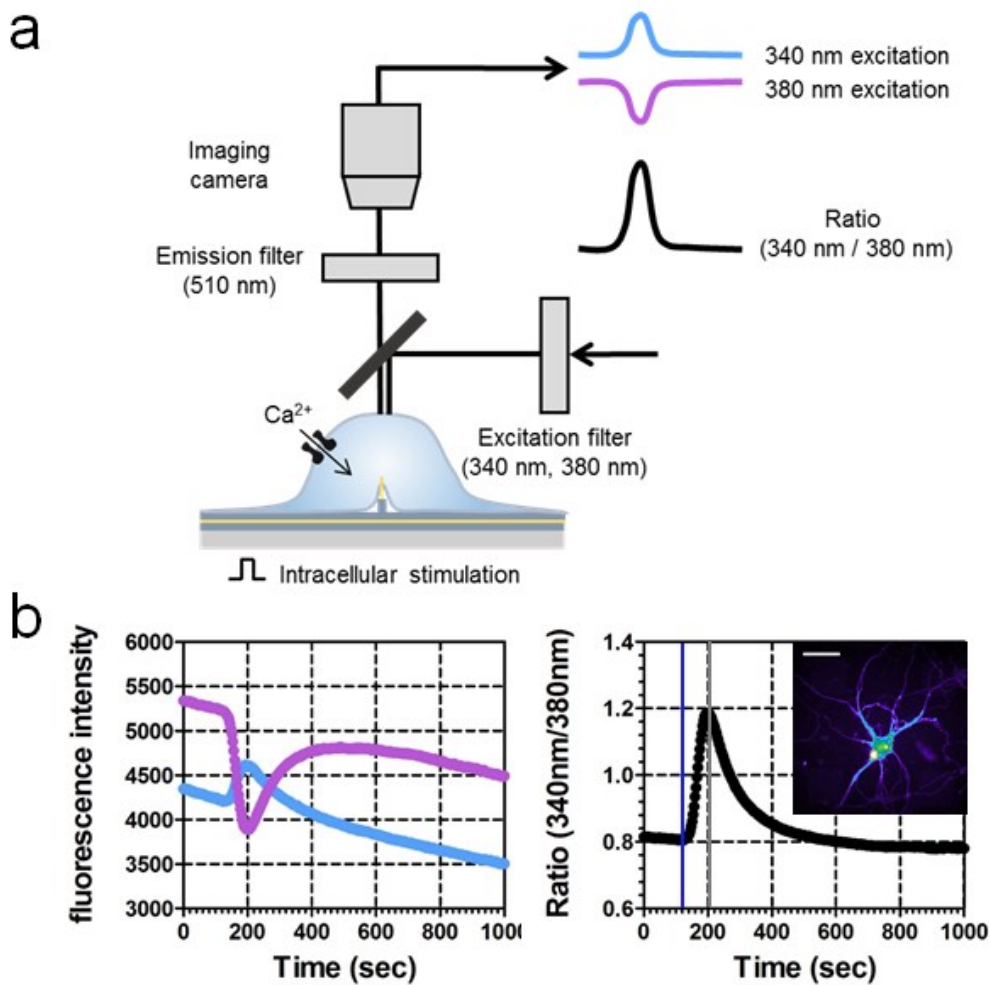


Figure S10. Monitoring neuronal activation triggered by intracellular stimulation using ratiometric calcium measurements **a.** Experimental set-up of dual-wavelength (ratiometric) calcium measurement using alternating excitation wavelengths (340 nm and 340 nm). The elevation of Ca²⁺ concentration in cells induces an increase in Fura-2 emission fluorescence at 340 nm and a decrease at 380 nm. **b.** Time-course of changes in the fluorescence intensity and ratio of Fura-2 during KCl-induced depolarization. Blue solid line in ratio graph indicates the time point of stimulus, and the grey line indicates that of KCl-wash out. (Inset image; Fura-2 fluorescence image of hippocampal neuron stimulated by KCl. Scale bar, 20 μ m.)

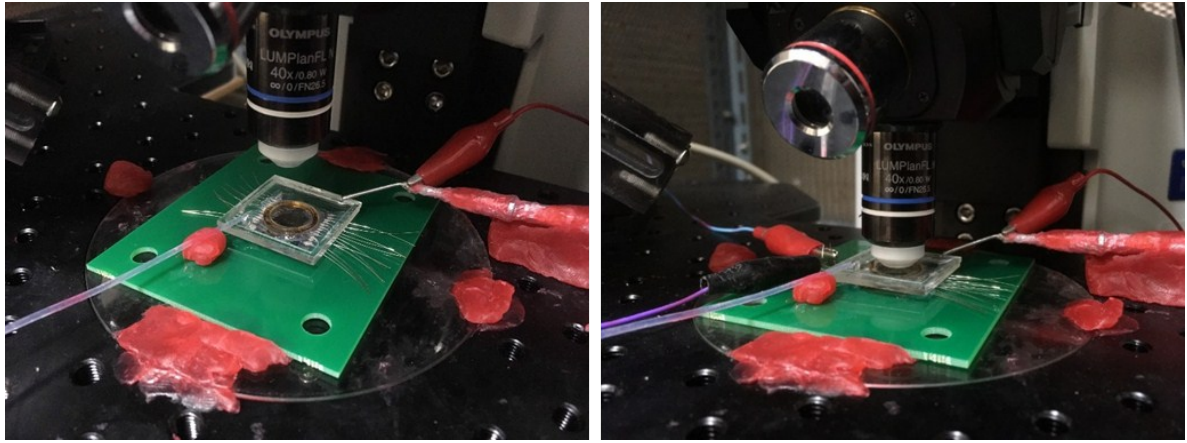


Figure S11. Live cell stimulation and imaging set-up. 64 stimulation pads of VNMEA are independently addressed electrically with a 0.2-mm silver wire. Cells were imaged through a 40x objective, using a charge-coupled device camera. Excitation was measured at 340 and 380 nm with a 150 W xenon lamp, and images were collected at 510 nm using Metaflour software (Molecular Devices).

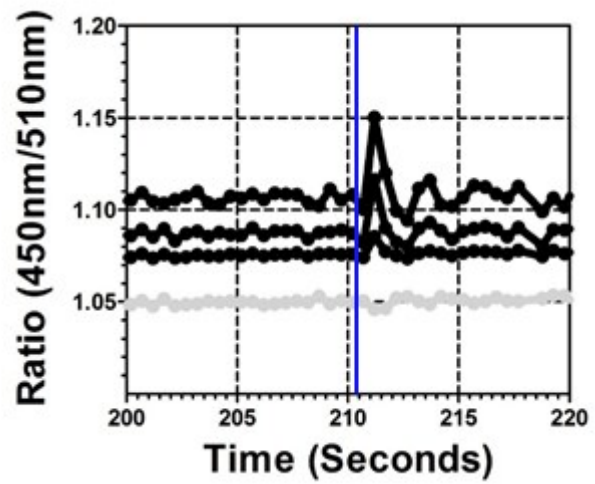
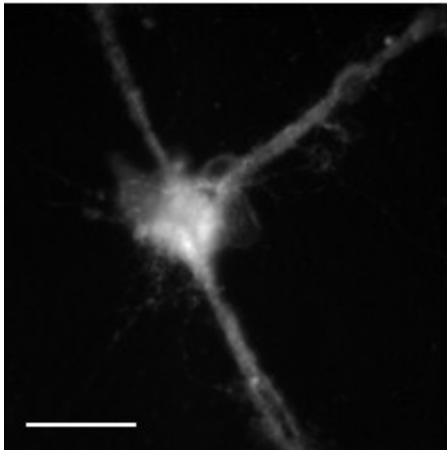


Figure S12. Detection of calcium transients associated with intracellular stimulus using a voltage-sensitive dye (VSD). VSD signals are monitored by membrane potential change of hippocampal neurons induced by intracellular stimulation (100 μ A, 10 ms). Scale bar, 50 μ m.

References

- 1 I. Kim, H. Y. Lee, H. Kim, E. Lee, D. W. Jeong, J. J. Kim, S. H. Park, Y. Ha, J. Na, Y. Chae, S. Yi and H. J. Choi, *Nano Lett.*, 2015, **15**, 5414–5419.
- 2 J. Lee, M. H. Hong, S. Han, J. Na, I. Kim, Y. J. Kwon, Y. beom Lim and H. J. Choi, *Nanoscale Res. Lett.*, 2016, **11**, 1–7.
- 3 I. Kim, S. E. Kim, S. Han, H. Kim, J. Lee, D. W. Jeong, J. J. Kim, Y. beom Lim and H. J. Choi, *Nanoscale Res. Lett.*, 2013, **8**, 1–7.